Arabian Journal of Chemistry (2023) **16**, 105049

King Saud University

Arabian Journal of Chemistry

www.ksu.edu.sa
www.sciencedirect.com

ORIGINAL ARTICLE

Adsorption and degradation of rhodamine B and bromocresol green by FeOCl under advanced oxidation process

Claudia Revilla Pacheco, Melani Ruth Riveros Cruz, Jaime Cárdenas Garcia, Ruly Terán Hilares *, Gilberto de Jesus Colina Andrade, David A. Pacheco Tanaka, Alejandra Mogrovejo-Valdivia

Laboratorio de Materiales, Facultad de Ciencias Farmacéuticas, Bioquímicas y Biotecnológicas, Universidad Católica de Santa María—UCSM, Urb. San José s/n—Umacollo, Arequipa 04000, Peru

Received 4 April 2023; accepted 31 May 2023
Available online 7 June 2023

KEYWORDS

Iron Oxychloride;
Fenton;
Photo-Fenton;
Photocatalysis;
Adsorption;
Ionic charge

Abstract FeOCl has gained popularity as a heterogeneous catalyst for pollutant removal in the Fenton process. However, humidification and adsorption of FeOCl are usually not considered in the process. In this way, the adsorption and Fenton activity using rhodamine B (RhB, cationic compound) and bromocresol green (BCG, anionic compound) as pollutants models, at various pH were studied (2, 3.6, 7, and 10). These studies show a very low adsorption level for RhB only at pH 10; therefore, the removal was due to the Fenton reaction. For BCG, at pH 10 the adsorption is almost zero, and at pH 7 after 240 min the adsorption was almost complete, at pH 7, the dye removal by adsorption is akin to Fenton, therefore, at this pH, the remotion was entirely attributed to adsorption. The solution's removal is the result of the adsorption and Fenton reaction. Additionally, the photocatalytic and photo-Fenton activity of FeOCl was studied by the removal of RhB from a solution at pH 3.6, removing about 84 and 95% of the dye respectively. Under these circumstances, FeOCl is a potential catalyst that could be used for Fenton, photo-Fenton, and photocatalysis. However, the present paper's experimental data shows that its activity depends largely on the percentage of humidity in the catalyst and the ionic charge of the contaminant that will be treated by the catalyst once it has been activated by water vapor. Characterization essays, such as XRD, show

* Corresponding author.
E-mail address: rteran@ucsm.edu.pe (R. Terán Hilares).
Peer review under responsibility of King Saud University.

Production and hosting by Elsevier

https://doi.org/10.1016/j.arabjc.2023.105049

a match for the synthesized FeOCl and FT-IR shows a peak change in the -OH groups range. This could be a possible explanation for the apparition of free radicals.

1. Introduction

Environmental pollution caused by the release of toxic compounds into water is an important issue nowadays and it is necessary to use synthesis methods that are cost-effective and do not involve the use of a lot of energy, as well as the use of precursors that are easy and inexpensive to obtain. Organic dyes are highly used by the textile, paper, leather, ink, ceramic, and cosmetic industry, they have the characteristic of being highly soluble and are discharged into freshwater. Due to their complicated structure, natural processes do not easily degrade them. Among the various methods for removing contaminants, are advanced oxidation processes (AOPs) which have shown great potential for degrading contaminants into small organic molecules, and mineralization into inorganic compounds, CO_2, and water. AOPs include cavitation, photolysis, photochemical reactions, photocatalysis, and Fenton and photo-Fenton reactions; the hydroxyl radical ($^{\bullet}OH$) is a strong oxidant and one of the most efficient specie which is typically responsible for the AOPs. Fenton oxidation is the most popular process because of its wide application range, strong anti-interference ability, simple operation, and rapid degradation (Hui Zhang et al., 2019; Kamble et al., 2023; Sarvalkar et al., 2021; Kamble and Ling, 2020). Conventional Fenton produces $^{\bullet}OH$ from H_2O_2 through the redox cycle of dissolved Fe(II)/Fe(III) species, however, it presents many challenges such as high chemical consumption, narrow pH working range, and significant production of iron oxyhydroxide sludge. Heterogeneous catalysis can overcome these limitations and also take advantage of an active surface to accelerate the formation of $^{\bullet}OH$ (Thomas et al., 2021; Zhu et al., 2019).

$^{\bullet}OH$ can also be generated from water using photocatalysts; the catalyst adsorbs a suitable wavelength light and an electron from the valence band is promoted to the conduction band forming electron-hole pairs, which migrate to the surface. The holes react with water producing $^{\bullet}OH$ as electrons react with dissolved O_2 in order to produce superoxide radical anions ($O_2^{\bullet-}$) which can react with water producing more $^{\bullet}OH$ (Zhu et al., 2019; Som et al., 2020). Different from TiO_2, the most common photocatalyst that uses UV radiation and also has the inconvenience of a large band gap (3.2 eV); iron hydroxides can work under solar radiation with subsequent reduction of operating costs (Hamd and Dutta, 2020). The photo-assisted Fenton process (photo-Fenton) has received great attention for removing emerging contaminants; the electrons generated by interaction with light, increase the Fe^{3+}/Fe^{2+} cycle rate in the Fenton process and promote the decomposition of H_2O_2 producing $^{\bullet}OH$, enhancing the catalytic degradation efficiency (Kamble et al., 2023; Li et al., 2022).

Iron oxychloride (FeOCl) is a heterogeneous catalyst that has shown excellent performance in the degradation of organic pollutants present in water at wide pH ranges and nowadays attempts have been made to support it into a membrane to avoid the costs for its reuse when the Fenton heterogeneous process has finished (Zhang et al., 2021). It is a layered material with strong in-plane chemical bonds with weak out-of-plane Van der Waals bonds between the layers; FeOCl is used as a host material of intercalation compounds because of its weak interaction between the layers (Zhang et al., 2016). The coordination bonds of Fe on the surface are the reactive centers where the H_2O_2 is linked. The coordination of electrophilic Cl^- and O is likely to increase the reduction potential of the exposed Fe, resulting in a more efficient single electron transfer from H_2O_2 (during the Fe(III) to Fe (II) reduction step) ***Figure S1***; as well as, a homolytic cleavage of H_2O_2 (Sun et al., 2018; Chen et al., 2021).

In most Fenton degradation studies using FeOCl reported in the literature, the catalyst is added to the solution containing the compound in order to degrade it and several minutes must pass so it can be adsorbed on the catalyst before H_2O_2 is added (Sun et al., 2018; Yang et al., 2013). The degradation degree is calculated from the concentration of analyte in the solution compared to the initial one which could be due to the adsorption or degradation by free radicals. The adsorption of the analyte will depend on its electrical charge and that of FeOCl at a given pH. Therefore, the pH and the adsorption must be considered as unequivocal elucidation of the reaction on heterogeneous Fenton catalysis, as cited by Cheng. et al (Chen et al., 2021) show for the first time, that FeOCl has an adsorption mechanism and does not just degrade contaminants for their removal (Hamd and Dutta, 2020).

In this work, FeOCl was synthesized, humidified, and then used for studies in adsorption and Fenton reaction at various pH by using Rhodamine B (RhB) and Bromocresol green (BCG) as cationic and anionic model substrates. The degradation of RhB was also studied under photochemical and photo-Fenton conditions.

2. Materials and methods

2.1. Reagents

Chemicals such as Rhodamine B, Bromocresol, Iron (III) chloride hexahydrate, hydrogen peroxide (30%) HNO_3, and NaOH were purchased from Merck® (Darmstadt, Germany).

2.2. Synthesis and characterization of iron oxychloride (FeOCl)

FeOCl catalyst was synthesized according to the thermal method reported by Sun et al. (Sun et al., 2018). First, the precursor $FeCl_3{\cdot}6H_2O$ was powdered and sieved with a 425 μm mesh size to obtain the most possible homogeneous particle size, then 3 g of sample powder was heated in a porcelain crucible at 220 °C with a heating rate of 10 °C. min^{-1}. The solid product was cleaned and shaken for 10 min and the solid was separated by centrifugation and filtered; this cycle was repeated 3 times with water and one more with ethanol. Then, the obtained catalyst was dried in an oven at 60 °C for 5 min (***Figure S2***). The catalyst was humidified by introducing FeOCl into a closed chamber saturated with water vapor for 24 h. The beaker was placed on a hot plate and kept at 55 °C for over 2 h and then at room temperature for 24 h. The water adsorbed by the catalyst on the humectation was determined by the weight loss at 106 °C using the Mettler Toledo HE73 moisture.

The XRD diffraction spectra of the FeOCl was obtained using a Miniflex 600-Rigaku X-ray diffractometer. FTIR spectra of the dry and humidified FeOCl (as pellets with KBr) were obtained using a Nicolet Summit OA- Thermo Scientific using KBr pellets. Zeta potentials were measured using a Zetasizer (Malvern), 30 mg of the humidified FeOCl was suspended in water and sonicated with a probe sonicator for 30 min after cooling, and another 30 min sonication was applied; then, pHs were adjusted using NaOH 0.05 N or HNO_3 0.05 N.

The pKa was measured by the potentiometric titration method, 30 mg of humidified FeOCl was suspended in 100 mL of water, an initial pH was measured with a Jenway ™ pH meter (Model 3510), then 280 µL of HNO_3 1 N was added considering the molarity of the sample (first point of the potentiometric titration). The titration then started adding the NaOH 0.05 N gradually until reaching pH 10 approximately. The pKa of RhB and BCG were determined by the same method using, 100 mL of 0.0104 mM and 0.0573 mM respectively. 20 µL and 10 µL of $HNO_3$1 N was added at each dye at the first point of the titration to cover a wide range of pH.

For the adsorption and degradation studies, the concentration of the dye in the solution was measured using a UV–vis spectrophotometer ThermoScientifc™ (GENESYS 50).

2.3. Dye adsorption studies

100 mL of the dye (RhB 0.0104 mM or BCG 0.0573 mM) was introduced into conical flask and the pH adjusted using NaOH (0.05 N) or HNO_3 (0.05 N), then, 30 mg of the humidified FeOCl was added; the flask was protected from the light by wrapping with aluminum foil and placed in an orbital shaker which was also protected from the light and samples were obtained each 10 min until reach 90 min, then each 30 min until 4 h. The temperature was kept constant at 25 °C during the experiments.

2.4. Fenton reactions

The reaction was carried out in the dark using the same conditions as in the adsorption studies. 100 mL of the dye (RhB 0.0104 mM or BCG mM 0.0573) was introduced into a conical flask, then H_2O_2 (150 µL with a concentration of 88.24 mM) was added, and the pH adjusted as above. Time zero was taken when 30 mg of the humidified FeOCl was introduced into the solution. At the same time intervals for adsorptions, aliquots were withdrawn and placed in a 5 mL Eppendorf centrifuge tube (measured by weight) which contained 0.5 g of scavengers to stop the generation of hydroxyl radicals (phosphate buffer pH 7.0 for RhB, or 0.5 mL of ethanol at 96 % for BCG). Finally, all samples were centrifuged at 10 000 RPM for 12 min for the separation of possible catalyst suspended in the sample.

2.5. Photo-Fenton reactions

The procedure was similar as Fenton, but using a solar simulator (SciSun-300, SCIENCETECH). The samples were placed in a 5.5 cm diameter beaker and at 25 cm of the light-emitting plate.

2.6. Photocatalytic reactions

The procedure was alike the Photo-Fenton, but without the addition of H_2O_2.

The degradation % for all the tests was calculated by Eq (1):

$$\%\, degradation = \left(1 - \frac{A_t}{A_0}\right) \times 100\% \quad (1)$$

Where: A_t = absorbance at time 't' and A_0 = initial absorbance.

3. Results and discussion

3.1. Characterization and activation of synthesized FeOCl

Fig. 1 shows the XRD diffraction peaks of the synthesized FeOCl (red line) and the one obtained from the library data of the equipment (Software PDXL2). It can be observed that peak patterns match very well with the standard diffraction pattern indicating that FeOCl was successfully prepared.

Several batches of FeOCl were synthesized, however, under the same conditions, the Fenton properties of both dyes were not reproducible, even using FeOCl from the same batch at different days. The synthesis and degradation studies were carried out in Arequipa, Peru which is located at 2300 m above the sea level and has low annual average humidity of around 45%. The degree of hydration of hydrophilic materials before their utilization could be important to improve their properties, as previously reported for hydrophilic carbon molecular sieves membranes for gas separation by Pacheco Tanaka et. al. (Nordio et al., 2020). As, FeOCl is a layered hydrophilic material, water can be loaded between the layers; at low ambient humidity, the layers are stacked together decreasing the active surface area.

Both adsorbed water and humidification increase with time as is shown in ***Table S2***; after 24 h, the adsorption was constant. Therefore, with a gentle hydration, water intercalates increasing the active area and allowing water molecules to bonded directly to Fe ion which intervene in the catalytic reaction (***Figure S1***). Fig. 2 shows the FT-IR spectra of the catalyst before (dry) and after exposition to humidity. The main difference is observed in the humidified FeOCl in the region of 500 cm^{-1} assigned to the Fe-O vibration of the catalyst

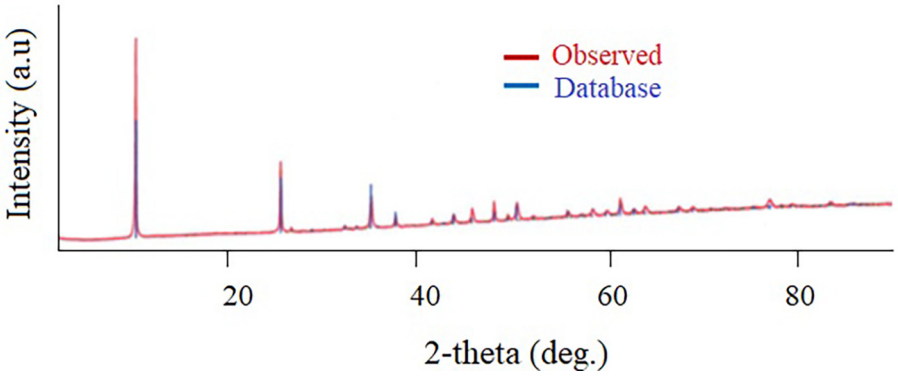

Fig. 1 XRD of FeOCl.

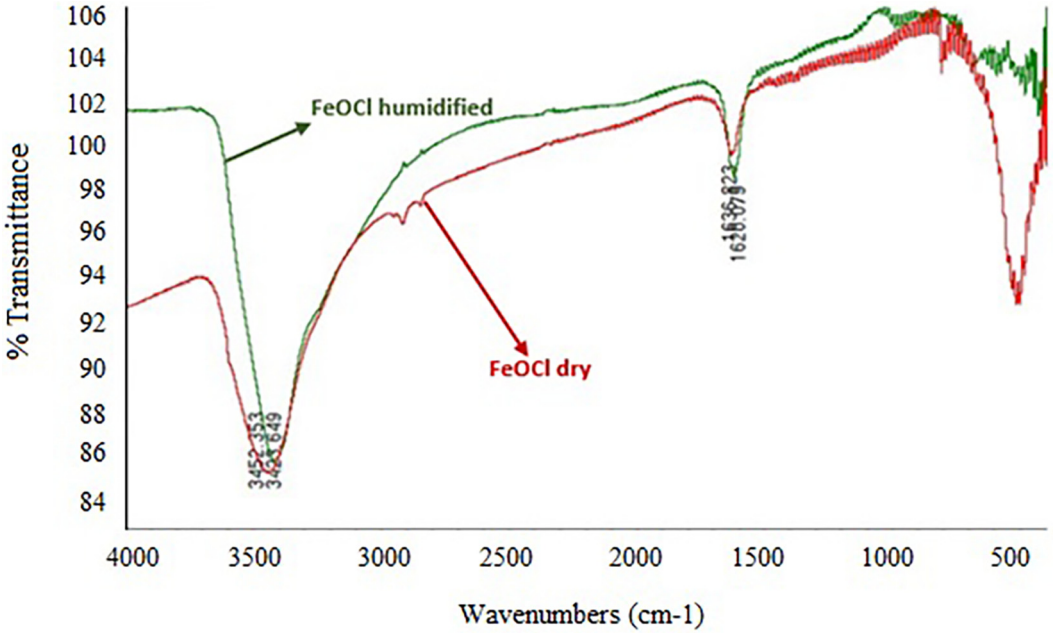

Fig. 2 FT-IR of FeOCl dry and humidified.

(Chen et al., 2021) which is responsible for the bond and free radicals formation from H_2O_2. The order parameter of the molecular orientation of water bonded to FeOCl will change with the pH since it will change the charge of the surface and the water rearrangement will change. It is expected that similar effect will occur with the refractive index and will affect the obtention of the complex refractive index from infrared reflectance spectroscopy.

The main disadvantage of the homogenous Fenton process is that the optimum pH value is between 2.8 and 3.5. At a pH < 2.8 in the heterogenous Fenton, the catalytic reaction occurs at the active site on the surface of the solid catalyst preventing the Fe ions from leaching, extending the working pH range, reducing the Fe sludge production and allowing the reuse of the catalyst (Hamd and Dutta, 2020). However, the $^{\bullet}OH$ production efficiency in the heterogenous system is inferior to its homogeneous counterpart due to mass transfer limitations and a reduced active surface area. Since the $^{\bullet}OH$ lifetime in water is extremely short (< 10 μs), its concentration in the bulk solution is much lower than the one on the surface of the catalyst where $^{\bullet}OH$ is produced (Zhang et al., 2020; Zhang et al., 2017; Duan et al., 2015). Heterogeneous reaction processes include interfacial H_2O_2 decomposition, possible active metal dissolution and organic adsorption (He et al., 2016). As FeOCl is a layered material with strong in-plane chemical bonds with weak out-of-plane Van der Waals bonds between the layers. The possibility of Fe dissolution is small, but it can be delaminated and released to the solution.

3.2. Zeta potential and pKa of FeOCl

The adsorption of organic compounds will be influenced by FeOCl surface's charge, which will depend on the pH. The zeta potential is related to the charge that develops at the interface between a solid surface and its liquid medium. The zeta potential of FeOCl with respect to the pH is shown in Fig. 3, the Zeta potential point zero charge (pH_{pzc}) is around 5.8. This result shows that pH values below 5.8 FeOCl will present a

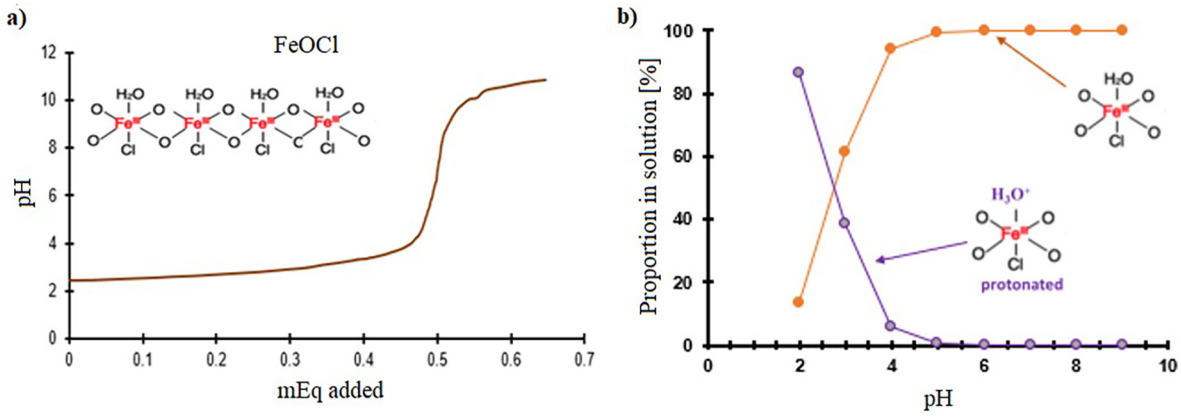

Fig. 3 Zeta potential of humidified FeOCl in the function of pH.

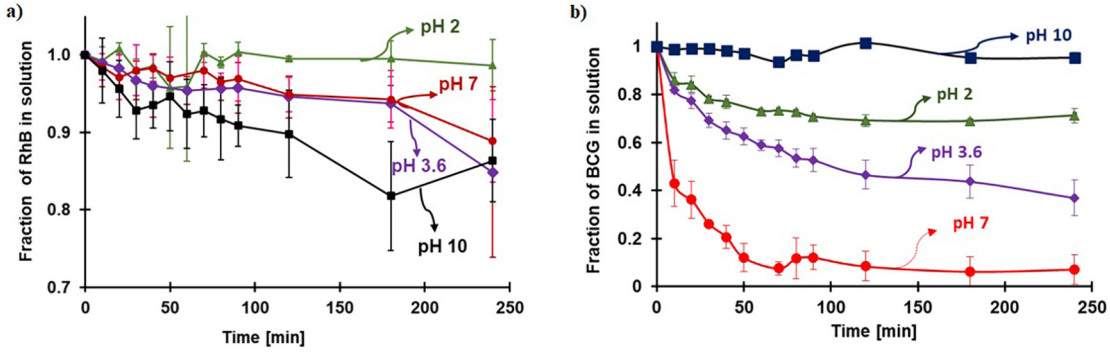

Fig. 4 a) potentiometric titration of FeOCl and b) Proportion of the protonated and deprotonated species concerning the pH.

positive charge on its surface, and above 5.8 pH values, the charge will be negative and the electrostatic attraction between FeOCl and the cationic state of the dyes will be promoted.

The pKa of FeOCl was obtained by the potentiometric titration method; the pH of the bulk solution with respect to mEq of NaOH added is presented in Fig. 4***a.*** The equivalent point is not exact (see first derivative plot ***Figure S3***) because all the Fe ions in it are not equivalent, and the laminates could have different sizes. The maximum point in the first derivative was used to calculate the pKa resulting in a value of 2.8. The proportion of protonated and deprotonated forms with respect to the pH of FeOCl is illustrated in Fig. 4***b***. It can be observed that it is related to the zeta potential graph (Fig. 3). The optimum pH for Fenton is the same as the pKa value for FeOCl (2.8); probably the H_2O_2 cannot replace the protonated water that is coordinating the Fe ion and the existence of the protonated form of H_2O_2 ($H_3O_2^+$).

3.3. Adsorption of RhB and BCG on FeOCl at different pH

To distinguish if the removal of the dyes from the solution is due to decomposition or the adsorption on the FeOCl surface, the adsorption of a cationic (Rhodamine B (RhB)) and an anionic (Bromocresol green (BCG)) were used as model compounds. The pKa of RhB and BCG were also experimentally determined by potentiometric titration (not reported here). The values found were 4.23, 4.79, respectively. These are close to those reported in the literature (Rather et al., 2022; Lamari et al., 2021). The structures of RhB and BCG are shown in ***Figure S4***, and the species concentration calculated from the pKa is listed in ***Table T1 and shown in Figure S5***. At pH 2, most RhB and FeOCl have been protonated (99.4 and 86.3 %, respectively). therefore, both species repel each other, preventing adsorption. At pH 3.6, 86.3% of FeOCl is charge-less and 81 % of RhB is positively charged, which means that some adsorption, due to ion–dipole interaction, is expected. Analogously, at pH 7 almost 100 % of FeOCl and RhB are in their neutral form. At pH 10, it is estimated that water coordinated to Fe can be deprotonated (forming a negative charge specie) and interacts with RhB's positive iminium group, so the highest adsorption is observed at this pH. Anyway, the adsorption of RhB is very small in the pH range studied.

As BCG is concerned, the adsorption is much higher than RhB except pH 10 where no adsorption occurs because both FeOCl and BCG (-2) are negatively charged. From all pH ranges studied, BCG is in the anionic form, at pH < 6 the two negatively charges species are present (***Table S1***). By changing the pH from 2 to 7, the percentage of BCG (-2), and the neutral FeOCl (FeOCl(0)) increases, and also the adsorption does. At pH 7, almost all dye had been adsorbed probably because of the complex formation between the Fe ion with the phenolate group of BCG. As the pH increases, FeOCl becomes negatively charged; thus, at pH 10, there is no adsorption.

3.4. Fenton, photofenton, and photocatalysis tests of FeOCl

One main difference between the homogeneous and heterogeneous Fenton catalysts is that the latter can be active at several pH levels. RhB and BCG removal at various pH levels in Fenton conditions are shown in ***Figure S7***; since FeOCl could have photocatalytic activity, Fenton experiments were carried out avoiding the presence of light in the reaction. The dye's removal from the solution can be due to adsorption from FeOCl and the degradation produced by the free radicals produced in the Fenton reaction. Therefore, the fraction of RhB (Fig. 5***a***) and BCG (Fig. 5***b***) removed from the solution by adsorption and in the Fenton process (adsorption and free-radical degradation) are shown in Fig. 6 ***and*** Fig. 7**,** respectively. For RhB, at pH 10, the adsorption is akin to Fenton degradation, probably, the adsorbed RhB on the surface inhibits the interaction between Fe ion and H_2O_2 (therefore the generation of $^{\bullet}OH$) (***Figure S1***). At other pHs, as the adsorption is very small, all the removals can be attributed to degradation from the Fenton reaction. For all the degradation kinetics, a pseudo-first-order model was applied since the H_2O_2 concentration is in a much higher proportion than the dye. The kinetics for the Fenton degradation of RhB is listed in Table 1; the reaction kinetics according to pH follows the $3.6 \gg 2 > 7$. By far, the fastest reaction is around pH 3.6 where the non-protonated FeOCl is mostly present, and the pH is still acidic.

As far as BCG is concerned, there is no adsorption at pH 10, therefore, the BCG removal is due to the Fenton reaction; yet among all the other pHs, the activity is the lowest, probably because H_2O_2 cannot easily coordinate with the negatively charged Fe-O^- groups in FeOCl. At high pH, the degradation rate decreases significantly because H_2O_2 is more susceptible to breaking down into H_2O and O_2 rather than forming free radicals. In addition to this, the potential oxidation of $^{\bullet}OH$ at

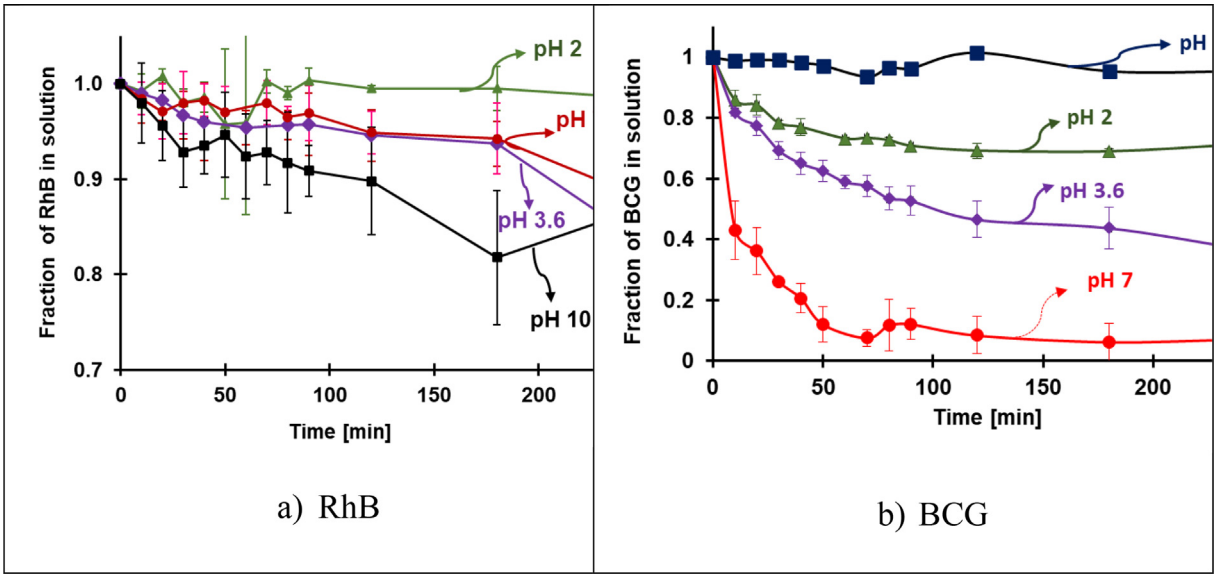

Fig. 5 Adsorption rate at pH 2,3.6, 7, and 10 of a) RhB and b) BCG. Conditions: 30 mg of FeOCl, initial concentration 0.0104 mM of RhB, and 0.0573 mM of BCG.

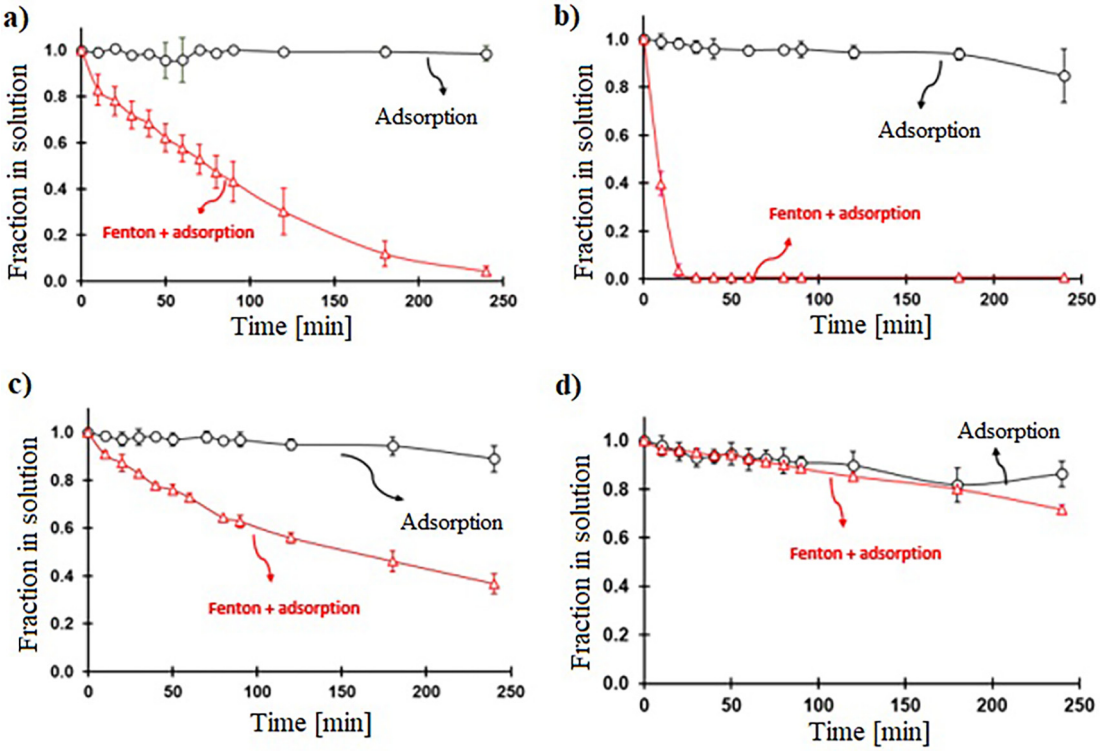

Fig. 6 Comparison of the remotion rates for Fenton (adsorption and free-radical degradation). 30 mg of FeOCl, initial concentration of RhB 0.0104 mM, and 49.0 mM of H_2O_2 and adsorption processes at various pH. a) pH 2, b) pH 3.6, c) pH 7 and d) pH 10.

high pH ($E° = 1.8$ V) is lower than the one in an acidic medium ($E° = 2.7/2.38$ V) (Hamd and Dutta, 2020). At pH7, the removal by adsorption is higher than Fenton's. The adsorption of BCG inhibits the interaction of H_2O_2 with the Fe ion, therefore, $^{\bullet}OH$ is not produced and the removal is mainly due to adsorption. At pH 3.6, adsorption is moderate, but the Fenton activity is very high; then the BCG is destroyed before forming the adsorption layer; and the free radicals are formed. Similar behavior occurs at pH 2.

The effect of the concentration of H_2O_2 during the time of degradation of RhB at pH 3.6 was studied and the results are displayed in Fig. 8. As expected, the degradation decreases alongside H_2O_2 concentration, however, there is not a clear pattern between them; probably, at lower concentrations, the

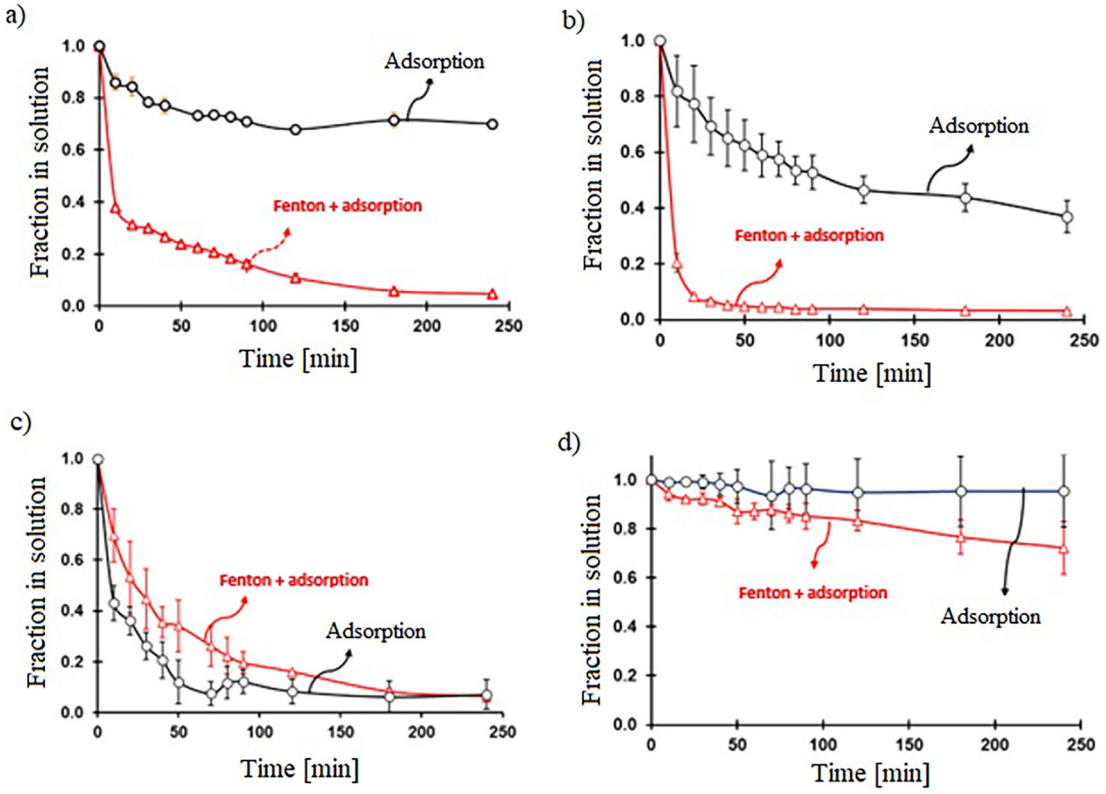

Fig. 7 Comparison of the remotion rates for Fenton (30 mg of FeOCl, initial concentration of BCG 0.0573 mM, and 49.0 mM of H_2O_2) and adsorption processes at various pH. a) pH 2, b) pH 3.6, c) pH 7 and d) pH 10.

Table 1 Pseudo first-order rate of the Fenton reaction for the degradation of RhB at various pHs.

pH	2.0	3.6	7.0	10
Rate [min $^{-1}$]	7.7	165.8	4.1	1.0

reaction does not behave as pseudo-first order, or there are other intermediate compounds that are not immediately destroyed.

Since the structure of humidified and dry FeOCl from the synthesis are not equal (Fig. 3), the percentage of water adsorbed at various humidification times was determined by gravimetry, and the results are shown in ***Table S2***. The water adsorbed increases with time, at 24 h, the gain was constant. The effect of the humidification time of FeOCl on the Fenton reaction was studied by the degradation of RhB at pH 3.6

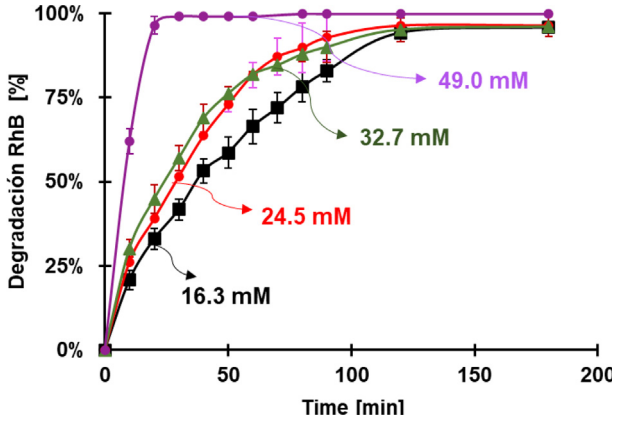

Fig. 8 Percentage of degradation of RhB at various concentrations of H_2O_2. Conditions: pH 3.6, 30 mg of FeOCl, dye concentration: 0.0104 mM of RhB.

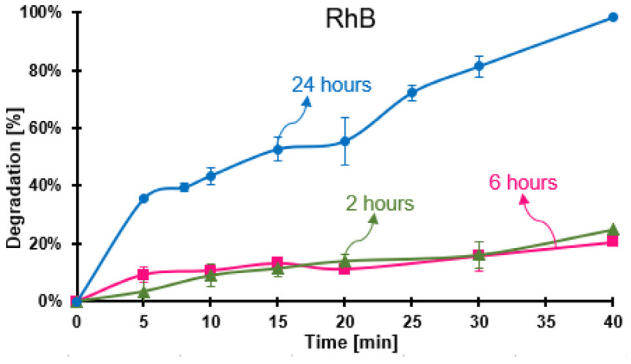

Fig. 9 Percentage of degradation of RhB by FeOCl humidified at different times. Conditions: pH 3.6, 30 mg of FeOCl, 0.520 mM for the initial concentration of RhB, and 49.0 mM of H_2O.

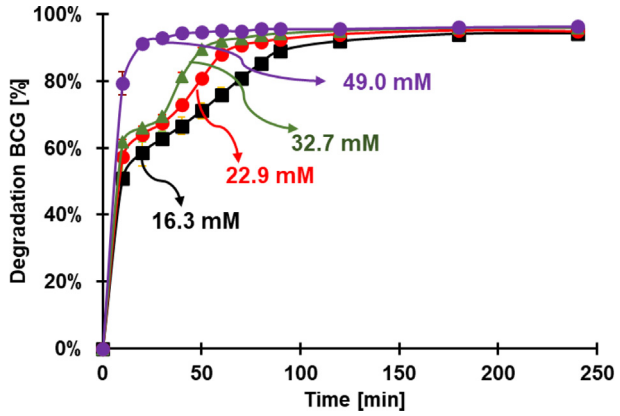

Fig. 10 Degradation of RhB at various concentrations of H_2O_2. Conditions: pH 3.6, 30 mg of FeOCl, initial concentration of RhB 0.0104 mM.

(Fig. 9), the highest activity was the one with the sample humidified for 24 h.

The Fenton activity of both dyes was under the same conditions (pH 3.6, 30 mg of FeOCl, 0.520 mM for the initial concentration of RhB and BCG, and 49.0 mM of H_2O_2) (***Figure S8***). The decomposition of BCG is faster than the one from RhB. This can be due to the higher adsorption of BCG (Fig. 7) compared to RhB (Fig. 6) at that pH. As a result, the •OH radicals formed during the Fenton reaction on the surface of FeOCl can promptly react with RhB. This cationic dye has very low interaction with the catalyst, therefore, the reaction will take place in the bulk solution, and the probability of reaction will be lower due to the short life of the free radicals in the media.

The effect of the concentration of H_2O_2 in the reaction (having all the other parameters constant (25 °C and no light) was evaluated in the degradation of RhB and BCG (Fig. 10). As it is expected, the degradation decreases with the concentration of H_2O_2, however, there is not a direct correlation between reaction rate and H_2O_2 concentration (***Table S3***), probably, because at lower concentrations, the reaction is not behaving as pseudo-first order, or because there are other intermediate compounds that are not immediately destroyed.

It was reported that the optical band gap E_g and the VB potential of FeOCl are 1.85 and 1.95 eV, respectively (Zhang et al., 2018), thus, this material has the possibility of having a photocatalytic activity. The photocatalytic degradation of RhB by FeOCl was studied because it cannot be adsorbed on the surface of the catalyst, increasing the possibility of the photon interacting with the valence electrons of FeOCl, thus, the effect of the solar radiation can be observed more clearly. The effect of irradiance on the degradation of RhB regarding time is presented in ***Figure S9***. At 0.178 sun, the degradation is very slow, when the irradiation was increased to 0.652, the degradation was increased considerably, it passed from 8 to 74 % of degradation in only 10 min. Thus, for further studies, to have more time to obtain samples, the irradiation was set to 0.276 sun. The photocatalytic degradation of RhB at 0.276 suns and pH 3.6 is displayed in Fig. 11***a*** and

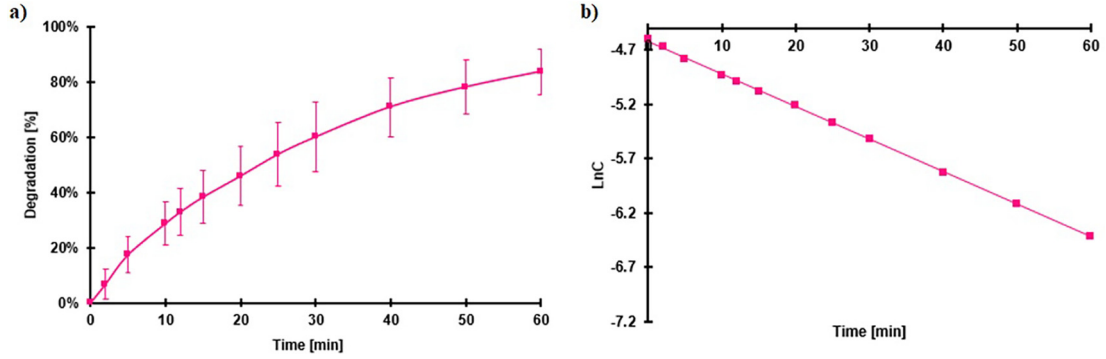

Fig. 11 a) Percentage of Photocatalytic degradation and b) pseudo-first-order degradation of RhB. Conditions 0.279 suns of irradiance, pH 3.6, 30 mg of FeOCl, initial concentration of RhB 0.0104 mM.

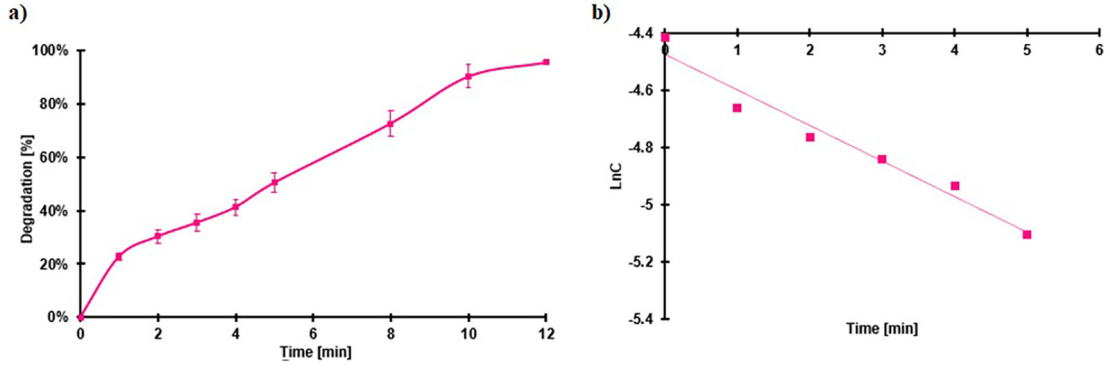

Fig. 12 Photo-Fenton degradation of RhB, a) percentage of degradation and b) kinetics degradation concerning time. Conditions: RhB 0.0104 mM, 6.52 mM H_2O_2, 0.279 suns of irradiance.

the pseudo-first-order degradation is in function of time in Fig. 11*b*. The kinetics of degradation obtained (k) is 0.03 min^{-1}.

As FeOCl has Fenton and Photocatalytic activity, the Photo-Fenton activity should be the combination of both. The concentration of H_2O_2 and the irradiation were used at a concentration of 6.52 mM and 0.279 sun respectively (to have enough time for sampling); the results are shown in Fig. 12.

For RhB, the degradation constant was 0.123 min^{-1}, which is like the Fenton degradation test with 48.97 mM H_2O_2 (0.166 min^{-1}), however; the dose of the oxidizing agent used was almost 7 times less. A higher amount of $^{\bullet}OH$ radical is generated because they are produced from the Fenton reaction and photocatalysis.

4. Conclusions

FeOCl, a heterogeneous Fenton catalyst was synthesized and characterized by FT-IR, XRD, and Zeta potential, noticing that the catalyst was properly synthesized and has a potential charge that adsorbs anionic dyes into its surface, this process is also a part of the contaminant removal by the catalyst. It was noticed that the Fenton activity was not reproducible even if the same sample were to be used on different days. This problem was solved by humidifying the sample 24 h before the catalytic test, showing a two-fold improvement in its degradation activity. The Fenton activity was studied in the dark using a cationic (Rhodamine B, RhB) and an anionic (Bromocresol green, BCG) dye as model compounds. In Fenton studies, the removal of the dye from the solution could be due to degradation by the Fenton reaction with free radicals and the adsorption by the heterogeneous catalyst. It was demonstrated that FeOCl has photocatalytic activity by studying the removal of RhB from a solution at pH 3.6, the removal increases with the irradiance of a solar simulator, and the degradation was increased considerably at photo-Fenton conditions since the amount of H_2O_2 used in Fenton is reduced. FeOCl is a potential catalyst that could be used by the textile, paper, leather, cosmetic, and other industries that use dyes as a treatment before it is discharged into rivers or lakes in a batch form or supported into a membrane as previously stated. However, a more in-depth study should be carried out to better understand the changes and activation of this catalyst under humidification conditions.

CRediT authorship contribution statement

Claudia Revilla Pacheco: Methodology, Investigation, Visualization, Writing – original draft. **Melani Ruth Riveros Cruz:** Investigation, Writing – original draft. **Jaime Cárdenas Garcia:** Visualization. **Ruly Terán-Hilares:** Writing – review & editing. **Gilberto de Jesus Colina Andrade:** Writing – review & editing. **David A. Pacheco Tanaka:** Writing – original draft, Writing – review & editing. **Alejandra Mogrovejo-Valdivia:** Supervision, Funding acquisition, Writing – original draft, Writing – review & editing.

Declaration of Competing Interest

The authors declare that they have no known competing financial interests or personal relationships that could have appeared to influence the work reported in this paper.

Acknowledgments

This study was supported by the Universidad Católica de Santa María (UCSM)- Peru. Grant No 27853-R-2021. The authors are grateful to Ph.D. Rita Nieto Montesinos and MSc. Derly Ortiz Romero from the Universidad Católica de Santa María – Arequipa, Peru.

Ethical approval

All authors certify that no human experiments were used.

Appendix A. Supplementary material

The submitted version contains supplementary material which includes the chemical structures of the catalyst and the kinetic degradation of RhB and BCG. Supplementary data to this article can be found online at https://doi.org/10.1016/j.arabjc.2023.105049.

References

Chen, Y., Miller, C.J., Collins, R.N., Waite, T.D., 2021. Key considerations when assessing novel Fenton catalysts: Iron oxychloride (FeOCl) as a case study. Environ. Sci. Technol. 55, 13317–13325. https://doi.org/10.1021/acs.est.1c04370.

Chen, L., Zuo, S., Guan, Z., Xu, H., Xia, D., Li, D., 2021. The practical application and electron transfer mechanism of SR-Fenton activation by FeOCl. Res. Chem. Intermed. 47, 795–811. https://doi.org/10.1007/s11164-020-04298-2.

Duan, X., Sun, H., Kang, J., Wang, Y., Indrawirawan, S., Wang, S., 2015. Insights into heterogeneous catalysis of persulfate activation on dimensional-structured nanocarbons. ACS Catal. 5, 4629–4636. https://doi.org/10.1021/acscatal.5b00774.

Hamd, W.S., Dutta, J., 2020. Heterogeneous photo-Fenton reaction and its enhancement upon addition of chelating agents. In: Nanomater. Detect. Remove. Wastewater Pollut., Elsevier Inc., pp. 303–330. https://doi.org/10.1016/B978-0-12-818489-9.00011-6.

He, J., Yang, X., Men, B., Wang, D., 2016. Interfacial mechanisms of heterogeneous Fenton reactions catalyzed by iron-based materials: A review. J. Environ. Sci. (China) 39, 97–109. https://doi.org/10.1016/j.jes.2015.12.003.

hui Zhang, M., Dong, H., Zhao, L., xi Wang, D., Meng, D., 2019. A review on Fenton process for organic wastewater treatment based on optimization perspective. Sci. Total Environ. 670, 110–121. https://doi.org/10.1016/j.scitotenv.2019.03.180.

Kamble, G.S., Ling, Y.C., 2020. Solvothermal synthesis of facet-dependent BiVO4 photocatalyst with enhanced visible-light-driven photocatalytic degradation of organic pollutant: assessment of toxicity by zebrafish embryo. Sci. Rep. 10, 1–11. https://doi.org/10.1038/s41598-020-69706-4.

Kamble, G.S., Natarajan, T.S., Patil, S.S., Thomas, M., Chougale, R. K., Sanadi, P.D., Siddharth, U.S., Ling, Y.C., 2023. BiVO4 as a sustainable and emerging photocatalyst: Synthesis methodologies, engineering properties, and its volatile organic compounds degradation efficiency. Nanomaterials 13. https://doi.org/10.3390/nano13091528.

Lamari, R., Benotmane, B., Mezali, S., 2021. Zeolite imidazolate framework-11 for efficient removal of bromocresol green in aqueous solution, isotherm kinetics, and thermodynamic studies. Desalin. Water Treat. 224, 407–420. https://doi.org/10.5004/dwt.2021.27183.

Li, J., You, J., Wang, Z., Zhao, Y., Xu, J., Li, X., Zhang, H., 2022. Application of α-Fe2O3-based heterogeneous photo-Fenton catalyst in wastewater treatment: A review of recent advances. J. Environ. Chem. Eng. 10,. https://doi.org/10.1016/j.jece.2022.108329 108329.

Nordio, M.L.V., Medrano, J.A., Van Sint Annaland, M., Tanaka, D. A.P., Tanco, M.L., Gallucci, F., 2020. Water adsorption effect on

carbon molecular sieve membranes in H2-CH4mixture at high pressure. Energies. 13. https://doi.org/10.3390/en13143577.

Rather, M.Y., Shincy, M., Sundarapandian, S., 2022. Photocatalytic degradation of Rhodamine-B by photosynthesized gold nanoparticles. Int. J. Environ. Sci. Technol. https://doi.org/10.1007/s13762-022-04123-w.

Sarvalkar, P.D., Mandavkar, R.R., Nimbalkar, M.S., Sharma, K.K., Patil, P.S., Kamble, G.S., Prasad, N.R., 2021. Bio-mimetic synthesis of catalytically active nano-silver using Bos taurus (A-2) urine. Sci. Rep. 11, 1–18. https://doi.org/10.1038/s41598-021-96335-2.

Som, I., Roy, M., Saha, R., 2020. Advances in nanomaterial-based water treatment approaches for photocatalytic degradation of water pollutants. ChemCatChem. 12, 3409–3433. https://doi.org/10.1002/cctc.201902081.

Sun, M., Chu, C., Geng, F., Lu, X., Qu, J., Crittenden, J., Elimelech, M., Kim, J.H., 2018. Reinventing Fenton chemistry: Iron oxychloride nanosheet for pH-insensitive H2O2 activation. Environ. Sci. Technol. Lett. 5, 186–191. https://doi.org/10.1021/acs.estlett.8b00065.

Thomas, N., Dionysiou, D.D., Pillai, S.C., 2021. Heterogeneous Fenton catalysts: A review of recent advances. J. Hazard. Mater. 404,. https://doi.org/10.1016/j.jhazmat.2020.124082 124082.

Yang, X.J., Xu, X.M., Xu, J., Han, Y.F., 2013. Iron oxychloride (FeOCl): An efficient Fenton-like catalyst for producing hydroxyl radicals in degradation of organic contaminants. J. Am. Chem. Soc. 135, 16058–16061. https://doi.org/10.1021/ja409130c.

Zhang, S., Hedtke, T., Zhu, Q., Sun, M., Weon, S., Zhao, Y., Stavitski, E., Elimelech, M., Kim, J.H., 2021. Membrane-confined iron oxychloride nanocatalysts for highly efficient heterogeneous fenton water treatment. Environ. Sci. Technol. 55, 9266–9275. https://doi.org/10.1021/acs.est.1c01391.

Zhang, J., Jiao, X.L., Xia, Y.G., Liu, F.F., Pang, Y.P., Zhao, X.F., Chen, D.R., 2016. Enhanced catalytic activity in liquid-exfoliated FeOCl nanosheets as a Fenton-like catalyst. Chem. - A Eur. J. 22, 9321–9329. https://doi.org/10.1002/chem.201600172.

Zhang, S., Quan, X., Wang, D., 2017. Fluorescence microscopy image-analysis (FMI) for the characterization of interphase HO• production originated by heterogeneous catalysis. Chem. Commun. 53, 2575–2577. https://doi.org/10.1039/c6cc09536d.

Zhang, S., Sun, M., Hedtke, T., Deshmukh, A., Zhou, X., Weon, S., Elimelech, M., Kim, J.H., 2020. Mechanism of heterogeneous fenton reaction kinetics enhancement under nanoscale spatial confinement. Environ. Sci. Technol. 54, 10868–10875. https://doi.org/10.1021/acs.est.0c02192.

Zhang, J., Zhao, X., Zhong, M., Yang, M., Lian, Y., Liu, G., Liu, S., 2018. An iron oxychloride/reduced graphene oxide heterojunction with enhanced catalytic performance as a photo-fenton catalyst. Eur. J. Inorg. Chem. 2018, 3080–3087. https://doi.org/10.1002/ejic.201800180.

Zhu, Y., Zhu, R., Xi, Y., Zhu, J., Zhu, G., He, H., 2019. Strategies for enhancing the heterogeneous Fenton catalytic reactivity: A review. Appl. Catal. B Environ. 255,. https://doi.org/10.1016/j.apcatb.2019.05.041 117739.